Pergamon

Int. J. Heat Mass Transfer. Vol. 40, No. 7, pp. 1657–1666, 1997

0017–9310/97 $17.00+0.00

PII: S0017–9310(96)00239–6

Pool boiling of R-22, R-124 and R-134a on a plain tube

CHUNG-BIAU CHIOU and DING-CHUNG LU

Department of Mechanical Engineering, National Chiao Tung University, Hsinchu 300, Taiwan, Republic of China

and

CHI-CHUAN WANG†

Energy & Resources Laboratories, Industrial Technology Research Institute, Hsinchu 310, Taiwan, Republic of China

(*Received* 20 *March* 1996)

Abstract—Pool boiling heat transfer on a plain tube having R-22, R-124 and R-134a as working fluids are reported in the present investigation. Experiments are conducted at saturation temperatures of 4.4°C and 26.7°C and at reduced pressures of 0.1 and 0.2. It is shown that the Cooper correlation can predict the present pool boiling heat transfer data satisfactorily. In addition, a semi-analytical prediction method is proposed in this study; this semi-analytical model can not only predict the present data with success, but also give reasonably good accuracy with the experimental data from other researchers. Copyright © 1996 Elsevier Science Ltd.

INTRODUCTION

Nucleate boiling heat transfer is a widespread industrial process. The importance of nucleate boiling arises from its ability to remove enormous quantities of heat per unit time and area from hot surface with a relatively low thermal temperature difference. This suggests a tremendous reduction in heat exchanger surface is likely by means of nucleate boiling. In recent years, significant progress has been made toward the understanding of nucleate boiling heat transfer, and correlations has been developed in order to precisely design flooded evaporators. However, it is still very difficult to predict boiling heat transfer coefficients with satisfactory accuracy. As illustrated by Stephan and Abdelsalam [1], many of the existing heat transfer data in nucleate boiling are inconsistent with each other. Cooper [2] argued that there is no agreement on the problem of relating heat flux to driving temperature potential. Recently, Kolev [3] examined experimental data for boiling of water on plain surfaces from 14 separate investigators. These investigators had reported about 5–6% error for temperature measurements and approximately 1–14% deviation for heat transfer measurements. However, Kolev [3] showed that the spread of the heat transfer data from different authors is over two orders of magnitude, which cannot be explained by measurement error. Therefore, it is essential to incorporate the correct physical mechanism of boiling heat transfer and the corresponding surface characteristics, to interpret the nucleate boiling heat transfer.

The ability to predict nucleate boiling heat transfer rates depends upon a knowledge of the mechanisms involved in the boiling heat transfer surface, and the growth and departure of the bubbles. There is no doubt that the growth and departure of the bubbles play an important role in the nucleation boiling heat transfer process. According to Mikic and Rohsenow [4], heat transfer by nucleate boiling is accomplished by the periodic removal of energy accumulated in the liquid that replaces the departing bubble, and hence, they concluded that the total heat flow rate $\dot{Q}$ at nucleate boiling can be separated into the heat flow $\dot{Q}_{mc}$ by microconvection and $\dot{Q}_{nc}$ by natural convection. This implies that the contribution of latent heat to total heat transfer is negligible. However, Blöchl [5] showed that the contribution of latent heat cannot be omitted especially for higher heat flux and higher reduced pressure; it is well known that the refrigerants used in refrigeration and air-conditioning industry generally fit into this category. Therefore, it is interesting to know the actual contribution of each heat transfer mechanism in the pool boiling process.

The main objective of the present study is to gain a better understanding of pool-boiling heat transfer through measuring the overall heat transfer coefficients of the R-22, R-134a, and R-124 refrigerants. Experimental results are compared with the modified Blöchl [5] semi-empirical model for pre-

† Author to whom correspondence should be addressed.

NOMENCLATURE

A	heat transfer area [m^2]
Cp	specific heat [J kg^{-1}]
D_b	bubble departure diameter [m]
D_0	outside diameter [m]
D_i	inside diameter [m]
f	bubble departure frequency [s^{-1}]
g	gravitational acceleration [m s^{-2}]
Gr	Grashof number
h	heat transfer coefficient [W m^{-2} K^{-1}]
i_{fg}	latent heat [kJ kg^{-1}]
Ja	Jacob number
Ja_m	modified Jacob number
k	wall thermal conductivity [W m^{-1} K^{-1}]
l	heating length [m]
M	molecular weight [kg $kmol^{-1}$]
N	bubble population
n	bubble density [m^{-2}]
P_c	critical pressure [kPa]
P_r	reduced pressure
Pr	Prandtl number
$\dot{Q}$	heat flow rate [W]
q''	heat flux [W m^{-2}]
R_p	surface roughness [μm]
r_c	critical radius [m]
T_{wall}	wall surface temperature [K]
T_{wi}	average inner wall temperature [k]
T_{w1}	top wall temperature [K]
T_{w2}	side wall temperature [K]
T_{w3}	bottom wall temperature [K]
T_{satl}	saturation temperature [K].

Greek symbols

ρ	density [kg m^{-3}]
σ	surface tension [N m^{-1}].

Subscripts

e	evaporation
f	fluid (liquid)
g	gas (vapor)
mc	microconvection
nc	natural convection
t	transient conduction
tot	total
w	wall.

dicting saturated nucleate boiling heat transfer rates, which included both the effects of the wall superheat and the effect of heat transfer surface characteristics.

EXPERIMENTALS

The schematic of the single-tube pool boiling apparatus is shown in Fig. 1(a). It consists of a cylindrical test vessel, a condenser and relevant connecting pipes made of stainless steel. Actually, the test setup is a natural circulation type apparatus. Heat is supplied to the tube by an internal cartridge heater, the evaporated vapor refrigerant leaves the test section through the vapor pipe line, and condensed in a separate condenser. The cylindrical boiling cell is made of stainless steel with a diameter of 88 mm and a length of 140 mm. The test vessel has a side- and a frontal-view window to observe the boiling phenomena.

The detailed geometries of the test tube is shown in Fig. 1(b). The length of the test tube is 100 mm and has an outside diameter of 17.8 mm. Inside the test tube, a cartridge heater with diameter of 5.8 mm and a length of 95 mm was installed in the test tube. The cartridge heater, having a maximum power of 670 W, is coated by magnesium oxide and is covered by a stainless steel. The stainless steel tube has a copper sleeve with three grooves to locate the thermocouples. Three T-type thermocouples are installed in the copper sleeve located at 50 mm from the flange to measure the temperature variations around the tube wall. Note that the location of the thermocouples are 90° apart as shown in Fig. 1(b).

A pressure gauge calibrated with an accuracy of $\pm 0.01\%$ is placed at the top of the test vessel to measure the system pressure. The liquid refrigerant temperature is recorded by two RTDs (resistance temperature device). All the thermocouples and RTDs were precalibrated by a quartz thermometer having a calibrated accuracy of 0.1°C. A high resolution power supplier capable of measuring the current of 0.01 A is used to provide the power source of the heater.

EXPERIMENTAL PROCEDURES

The test section was initially cleaned and leak free before it was evacuated using a turbo-molecular vacuum pump. The vacuum pump continued working for another 2 h after the vacuum gauge manometer reached 10^{-4} torr, to ensure that it contained no noncondensable gases, then the refrigerants were charged into the system.

Pool boiling experiments were conducted for refrigerants R-22, R-124, and R-134a at saturation temperatures of 4.4 and 26.7°C and at reduced pressures of 0.1 and 0.2. The liquid refrigerants were gradually preheated to its corresponding saturated state before running each test. Power was then adjusted to a prior setting. The criterion of steady state condition was the variation of system pressure

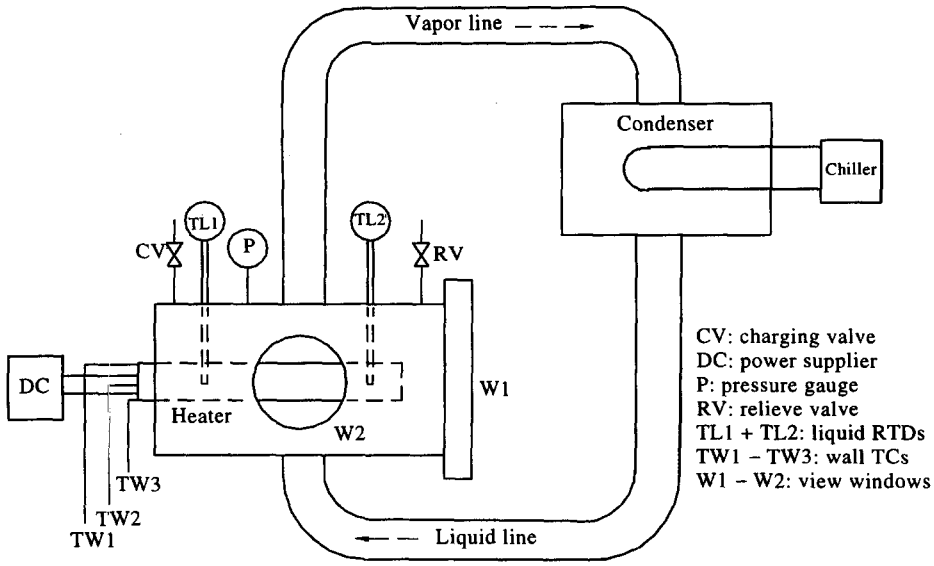

(a)

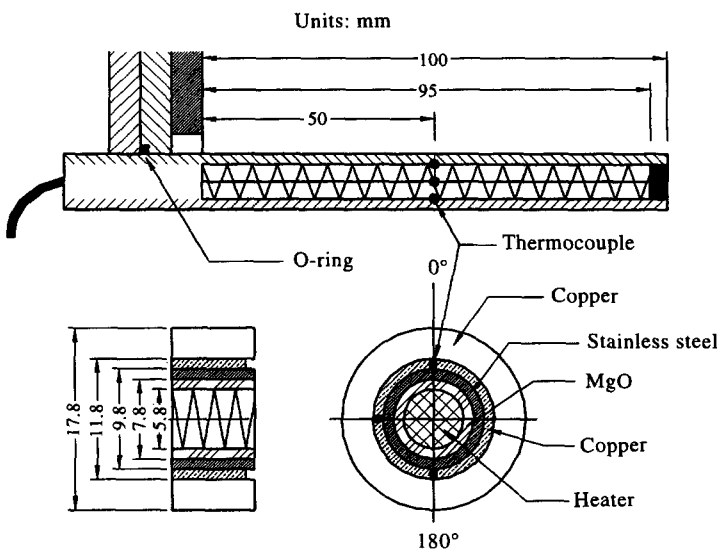

(b)

Fig. 1. (a) Schematic diagram of experimental setup; (b) detailed geometries of the test and test tube.

to be within ± 3 kPa and the temperature variations of the wall surface were less than ± 0.1°C over 5 min. All the data signals are collected and converted by a data acquisition system (a hybrid recorder). The data acquisition system then transmits the converted signals through GPIB interface to the host computer for further operation. The experimental uncertainties reported in the present investigation, following the single-sample method proposed by Moffat [6], are tabulated in Table 1. The maximum and minimum uncertainties of the heat transfer coefficients were estimated to be approximately 16.8% for $\dot{Q} = 2.6$ W and 1.37% for $\dot{Q} = 668$ W.

DATA REDUCTION AND EXPERIMENTAL RESULTS

The heat transfer coefficient for each power input was calculated as follows:

$$h = \frac{\dot{Q}}{A(T_{\text{wall}} - T_{\text{sat}})} \tag{1}$$

where $\dot{Q}$ is the electric heating power. T_{sat} is the saturation temperature based upon the measurement of system pressure. The outside surface area, A, is evaluated as $\pi D_0 l$. Note that D_0 is the outside tube diameter, and l is the length of the cartridge heater ($l = 95$ mm).

Table 1. Summary of estimated uncertainties

Primary measurements	Uncertainty	Derived quantities	$\dot{Q}=2.6$ W (minimum)	$\dot{Q}=668$ W (maximum)
l	10^{-3} m	ΔT	14.1%	0.94%
D_0	10^{-5} m	A	0.83%	0.83%
T	0.1°C	$\dot{Q}$	9.17%	0.57%
I	0.01 A	q''	9.21%	1.00%
V	1 V	h	16.8%	1.37%

T_{wall} is the mean average wall temperature at the outer surface, which can be calculated from the measurement of inside temperatures, and is given by

$$T_{wall} = T_{wi} - \dot{Q}\frac{\ln(D_0/D_i)}{2\pi k_w l} \quad (2)$$

where T_{wi} is the arithmetic mean of three inside wall temperatures:

$$T_{wi} = \frac{T_{w1} + 2T_{w2} + T_{w3}}{4} \quad (3)$$

where T_{w1}, T_{w2} and T_{w3} are the inside wall temperature readings, respectively.

Figure 2 shows the comparison of heat transfer coefficients vs heat flux for R-134a refrigerant between the present data and those of Webb and Pais [7]. The saturation temperatures shown in the figure are 4.4 and 26.7°C, respectively, which are identical to the test conditions of Webb and Pais [7]. As seen, the present data agree favorably with those of Webb and Pais [7]. Figure 2 also shows the heat transfer coefficients predicted by Cooper [8], Stephan and Abdelsalam [1], and Mostinski [9]. The Cooper [8] correlation is given as

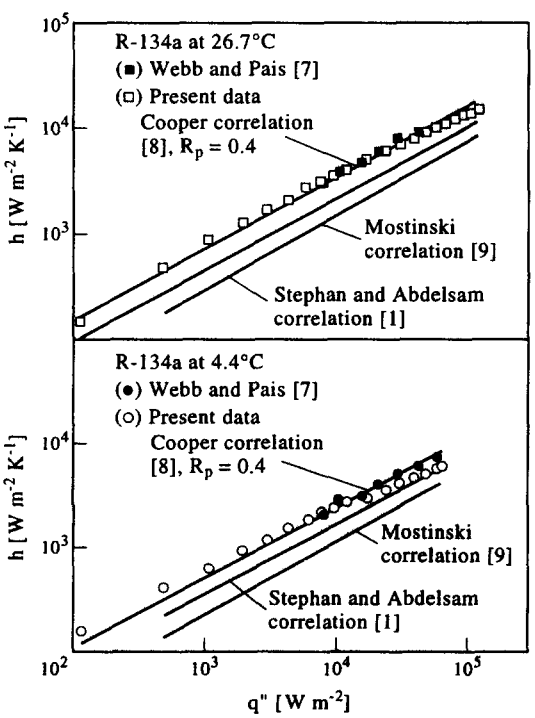

Fig. 2. Comparison of R-134a data with Webb and Pais [3] and correlations of Cooper [8], Stephan and Abdelsalam [1] and Mostinski [9].

$$h = 90(q'')^{0.67} M^{-0.5} P_r^m (-\log_{10} P_r)^{-0.55} \quad (4)$$

$$m = 0.12 - 0.2\log_{10} R_p. \quad (5)$$

As reported by Stephan and Abdelsalam [1], the commercial finish copper tubes generally have a surface roughness of 0.4 μm. Therefore, the surface roughness, R_p, is given as 0.4 μm in the present calculation. The choice of surface roughness, R_p, has little effect on heat transfer rate as depicted by Cooper [8]. It is shown that the present data agree closely with the Cooper correlation. A slight over-prediction of the Cooper correlation is found for a heat flux over 30 kW m^{-2}. One of the explanations is that the slope of the h vs q'' curve for the Cooper correlation (equation (4)) is independent of heat flux (0.67), and the present data indicate that the slope decreases a small amount for higher heat flux. The decrease of slope is much more noticeable for the enhanced tubes as illustrated by Webb and Pais [7]. For comparison purpose, the Stephan and Abdelsalam [1] correlation and the Mostinski correlation [9] are also drawn in the figure. As seen, the Stephan and Abdelsalam [1] correlation and the Mostinski [9] correlation considerably underpredict the experimental data. Generally, about 20–30% underpredictions for the Stephan and Abdelsalam [1] correlation are reported, and approximately 40–100% underpredictions for the Mostinski [9] correlation are shown. Webb and Pais [7] also reported an underprediction of 20–25% of the Stephan and Abdelsalam [1] correlation.

Figure 3 shows the heat transfer coefficients versus heat flux at reduced pressures of 0.1 and 0.2 for R-22, R-134a, and R-124. As seen in this figure, the deviations between the heat transfer coefficients are quite small for a given reduced pressure. This result reveals that the reduced pressure plays a significant role in correlating pool boiling heat transfer data. As seen in the Cooper correlation (equation (4)), the primary correlation parameter is the reduced pressure. Eventually, the Cooper [8] correlation can predict the present experimental data better than other correlations.

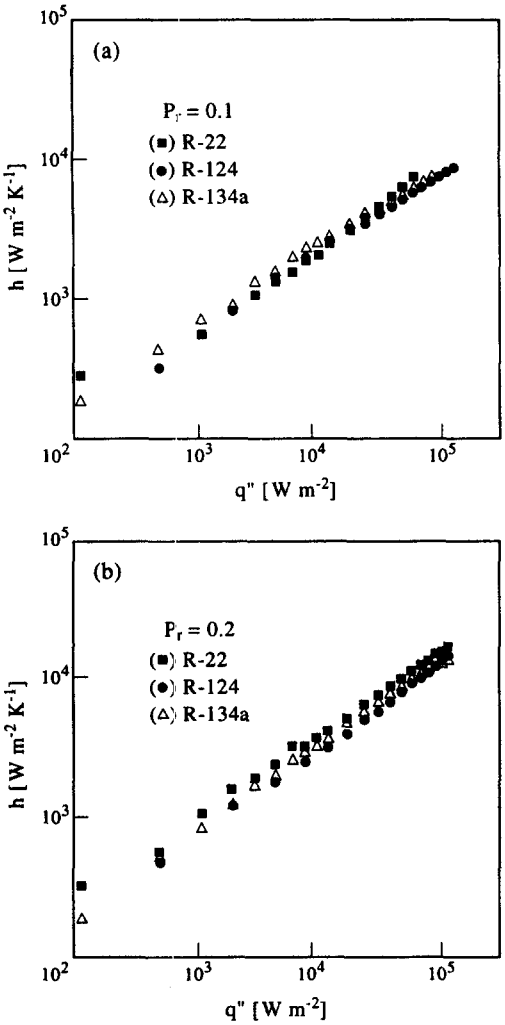

Fig. 3. Pool boiling data of R-22, R-124 and R-134a (a) at P_r = 0.1; (b) at P_r = 0.2.

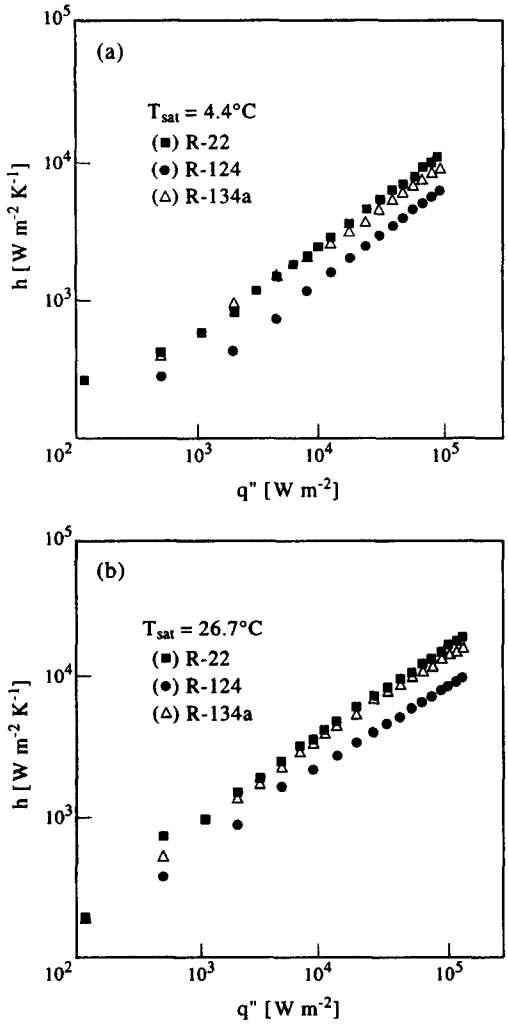

Fig. 4. Pool boiling data of R-22, R-124 and R-134a (a) at 4.4°C; (b) at 26.7°C.

Figure 4(a) and (b) presents the heat transfer coefficients versus heat flux at saturation temperatures at 4.4°C and 26.7°C, respectively. As seen, the heat transfer coefficients for R-124 are considerably lower than those of R-22 and R-134a. The main reason can be seen from the physical properties of the tested refrigerants illustrated in Table 2. For a prescribed saturation temperature, the corresponding saturation pressure for R-22 and R-134a are higher than that of R-124. As a result, higher heat transfer coefficients for R-22 and R-134a are seen.

Figure 5 show the photographs of nucleate boiling for refrigerants of R-22, R-134a and R-124 at reduced pressure of 0.1 and 0.2 at a heat flux of 49.3 kW m^{-2}. The increase of reduced pressure will decrease the bubble size and consequently the regime of isolated bubble will sustain at a higher heat flux. These figures show no significant distinctions between bubble size and frequency at the same reduced pressure.

Figure 6 shows the photographs of nucleate boiling at saturation temperature of 26.7°C and at heat fluxes of 12.2, 49.3 and 110.7 kW m^{-2} for R-22 and R-124. Examination of the pictures indicates that the flow pattern is in isolated bubble regime for a heat flux of 12.2 kW m^{-2}, and then moves to the regime of slugs and column at a heat flux of 110.7 kW m^{-2}. The number of active nucleation sites increase sharply with increasing heat flux. For a given heat flux, the size of the bubble diameter for R-22 is smaller than that of R-124. This is because, as indicated in Table 2, the reduced pressure for R-124 is 0.118 compared to 0.218 for R-22. Consequently, it is expected that the bubble size of R-124 is much larger than R-22.

MODELING OF HEAT TRANSFER

In the modeling of saturated pool boiling from an active bubble site, the heat transfer rate can be considered to be the sum of four principal components [10]. Namely, the contribution of microconvection due to bubble growth and departure, latent heat transport in the vapor bubble, natural convection and the

Table 2. Properties of tested refrigerants

	M (kg kmol^{-1})	P_c (kPa)	i_{fg} at 20°C (kW kg^{-1})	P_r $T_{sat}=4.4$°C	Reduced pressure $T_{sat}=26.7$°C	T_{sat}°C $P_r=0.1$	$P_r=0.2$
R-22	86.48	4990	187.28	0.114	0.218	0.23	23.54
R-124	136.47	3634	147.96	0.053	0.111	23.36	47.53
R-134a	102.03	4056	182.44	0.084	0.172	9.35	31.82

sensible heat transfer due to Marangoni flow. The fluid flow induced by the temperature-related surface tension gradient on a liquid/vapor interface is known as the thermocapillary or Marangoni flow. Theoretical calculations of the thermal contribution of Marangoni flow to the total heat flux is negligible, except in very high subcooling [10]. Therefore, it is not included in most theoretical analysis. Mikic and Rohsenow [4] suggested that the latent heat may not be a predominant factor in practical cases. Consequently, most previous investigations had divided pool boiling heat transfer into two mechanism, namely the contribution of microconvection and of natural convection:

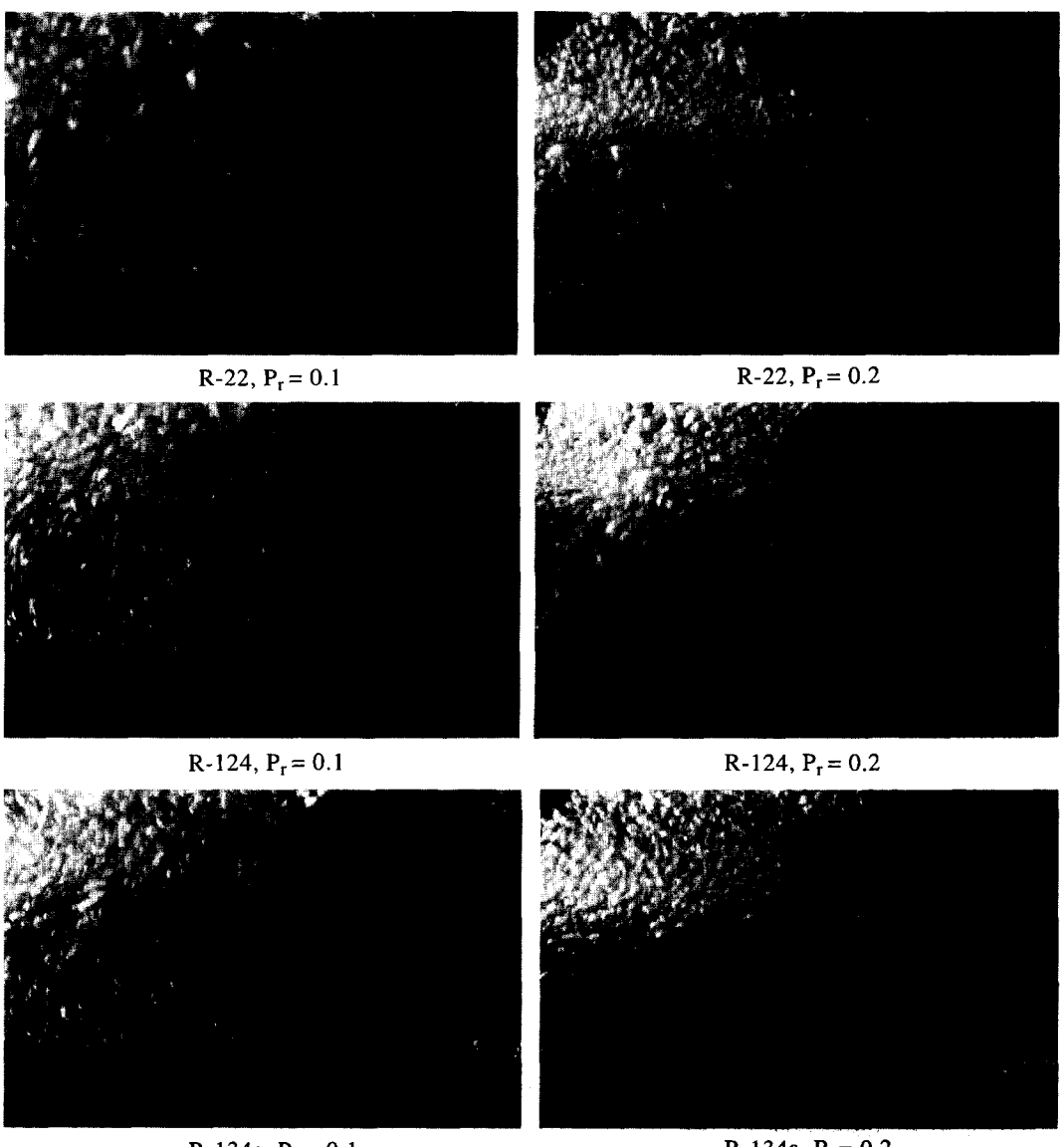

Fig. 5. Photographs of boiling phenomena at $P_r = 0.1$ and $P_r = 0.2$ and at $q'' = 49.3$ kW m^{-2} for R-22, R-124 and R-134a.

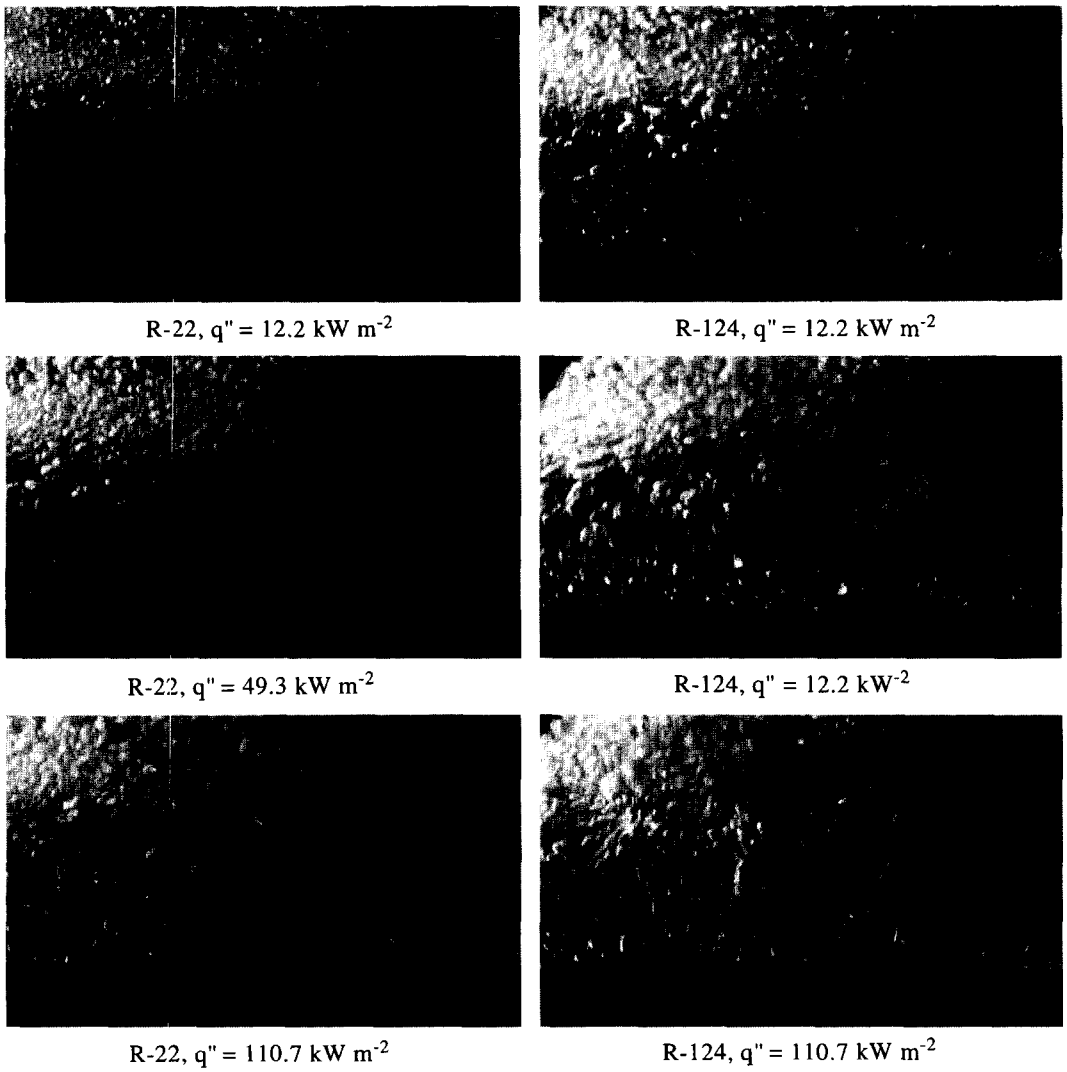

Fig. 6. Photographs of boiling phenomena at $T_{sat} = 26.7°C$ for R-22 and R-124 at $q'' = 12.2$, 49.3 and 110.7 kW m^{-2}.

$$\frac{\dot{Q}}{A} = h\Delta T = \frac{A_{mc}}{A}\bar{q}_{mc} + \frac{A_{nc}}{A}q_{nc} \tag{6}$$

where $\bar{q}_{mc}$ is the average of the microconvection heat flux over the time interval, and q_{nc} is due to natural convection heat flux. Using the conjugate error function solution to evaluate the heat flux from the surface to this region yields:

$$\bar{q}_{mc} = \frac{2}{\sqrt{\pi}}\sqrt{k_f\rho_f Cp_f}\sqrt{f}\Delta T = h_t\Delta T \tag{7}$$

$$A_{mc} = \pi N D_b^2 \tag{8}$$

$$A_{nc} = A - A_{mc} \tag{9}$$

therefore,

$$h_t = \frac{2}{\sqrt{\pi}}\sqrt{k_f\rho_f Cp_f}\sqrt{f}. \tag{10}$$

The contribution of natural convection, q_{nc}, is given by

$$q_{nc} = h_{nc}(T_{wall} - T_{sat}) \tag{11}$$

where h_{nc} is the heat transfer coefficient of natural convection from horizontal cylinder proposed by Bayley [11], i.e.

$$h_{nc} = \frac{k_f}{D}0.1(GrPr)^{(1/3)}. \tag{12}$$

Equation (7) suggests that the heat transfer in microconvection is only due to the transient conduction into the sublayer. This assumption was confirmed for boiling of water at low pressure. However, Blöchl [5] showed that the contribution of latent heat transfer to the total heat transfer rate cannot be neglected. He adds a second term to equation (7) for h_{mc} to take into account the latent heat transport effect resulting from

the superheated liquid evaporation at the surface of the bubbles:

$$h_{mc}\Delta T=\frac{2}{\sqrt{\pi}}\sqrt{k_f\rho_f Cp_f}\sqrt{f\Delta T}+\frac{1}{6}\rho_g i_{fg} f D_b = q_t''+q_e'' \tag{13}$$

where D_b and f are the bubble departure diameter and bubble departure frequency, respectively. To apply the above-mentioned model, information for the bubble departure diameter and bubble departure frequency must be available. The bubble diameter can be calculated using the Cole and Rohsenow correlation [12], and is given by

$$D_b = C(Ja_m)^{5/4}\sqrt{\frac{\sigma}{g(\rho_f-\rho_g)}} \tag{14}$$

$$Ja_m=\frac{T_{sat}Cp_f\rho_f}{\rho_g i_{fg}} \tag{15}$$

where

$$\left\{\begin{matrix} C=1.5\times10^{-4} & \text{for water} \\ C=4.65\times10^{-4} & \text{for other fluids}\end{matrix}\right\}.$$

The correlation for the prediction of bubble frequency used in the present investigation is taken from Zuber [13]:

$$fD_b = 0.59\left[\frac{\sigma g(\rho_f-\rho_g)}{\rho_f^2}\right]^{1/4}. \tag{16}$$

The active nucleation site density can be derived from equations (6), (7), (8) and (11):

$$\frac{N}{A}=n=\frac{1}{\pi D_b^2}\frac{h-h_{nc}}{h_{mc}-h_{nc}}. \tag{17}$$

A unique feature of Blöchl's [5] model is the way the active nucleate site density is determined from the size distribution of active nucleation cavities on the heat transfer surface. It is generally agreed [14–16] that the pool boiling active nucleation site density can be determined as a function of the cavity radius in the form

$$n = Cr_c^{m1} \tag{18}$$

where r_c is the minimum cavity radius at a specified condition, and is given by

$$r_c=\frac{2\sigma T_{sat}}{\rho_g i_{fg}\Delta T}. \tag{19}$$

The constants C and $m1$ in equation (18) characterize the boiling surface, and can be obtained from the experimental data.

Bier *et al.* [17] suggested an alternative form to represent the active nucleation distribution in the form of a Rosin–Rammler–Sperliling distribution:

$$\ln(N/A)=\ln(N/A)_{max}[1-(r_c/r_{max})^{m2}] \tag{20}$$

where r_{max} is the total number of the nucleation sites available on the heat transfer surface.

Based on their experimental data, Jamialahmadi *et al.* [18] proposed a simple exponential form:

$$\ln(N/A)=A_1+A_2r_c+A_3r_c^2. \tag{21}$$

Despite the fact that these previous works have achieved significant progress in theories, it seems that these forms cannot accurately reflect the dependence of the nucleation site density on the boiling surface conditions (Yang and Kim [19]). Kocamustafagullari and Ishii [20] indicated that equation (19) is difficult to use in practice. Generally, the empirical constants used in these above-mentioned equations are only applicable to their own data. It is noted that the active nucleation sites should depend upon other refrigerant properties such as surface tension. Therefore, an empirical form of active nucleation sites is developed based on the present R-22, R-134a, and R-124 to yield:

$$n=(e^z)/Ja^{1.2} \tag{22}$$

where

$$z=\frac{Y(1+M^{0.2})}{(1+P_r)(1.0-10\sigma)} \tag{23}$$

$$Y=640.93-45.87X+1.117X^2-2996/X \tag{24}$$

$$X=\ln(1/r_c) \tag{25}$$

$$Ja=\frac{Cp_f\rho_f\Delta T}{\rho_g i_{fg}}. \tag{26}$$

We then try to apply the correlation to predict experimental data from other researchers.

DISCUSSION OF THE MODEL

Figure 7(a) shows the heat transfer rate for the contributions of transient conduction, latent heat transport, and natural convection at a reduced pressure of 0.2 and of 0.01 for R-123. As seen, the latent heat transfer is the dominant heat transfer mechanism for a given reduced pressure of 0.2 and at a wall superheat less than 2°C. The contribution of transient conduction to total heat transfer increases sharply with the increase of wall superheat, and is comparable to latent heat transfer for a wall superheat of 5°C. The natural heat transfer does not show a noticeable increase vs wall superheat. Despite the increase of wall superheat results, an increase of the natural convection component, the natural convection heat flux, reveals maximum characteristics vs wall superheat. The reason for this phenomenon can be explained from the change of 'influence area' of departing bubbles. As shown in Fig. 6, the active bubble sites increase significantly with heat flux (wall superheat). Therefore, the 'influence area', A_{mc}, for a departing bubble is increasing with the wall superheat, and eventually reduces the surface area for natural con-

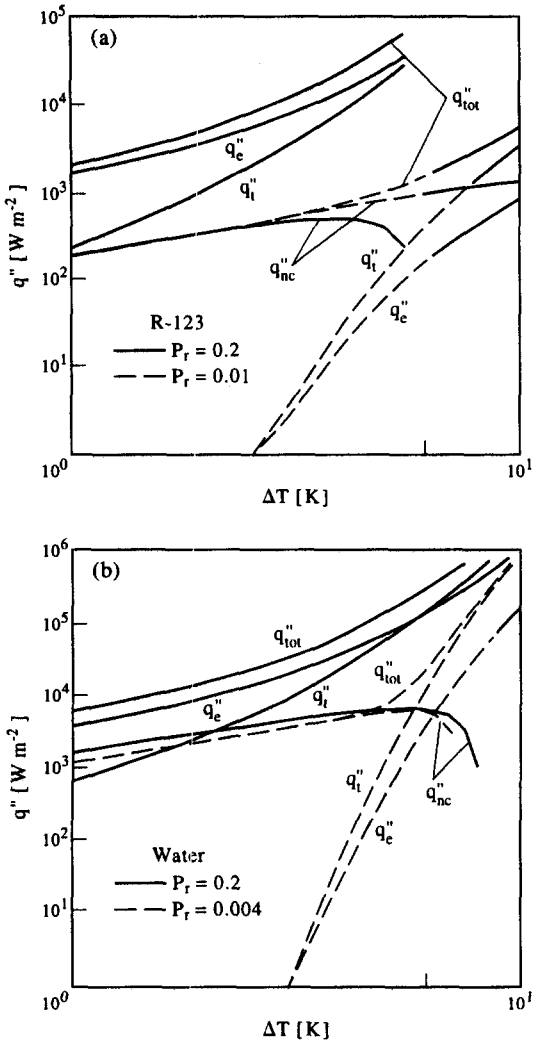

Fig. 7. The contributions of transient conduction, latent heat, and natural convection heat flux for (a) R-123 at $P_r = 0.2$ and $P_r = 0.01$; (b) water at $P_r = 0.2$ and $P_r = 0.01$.

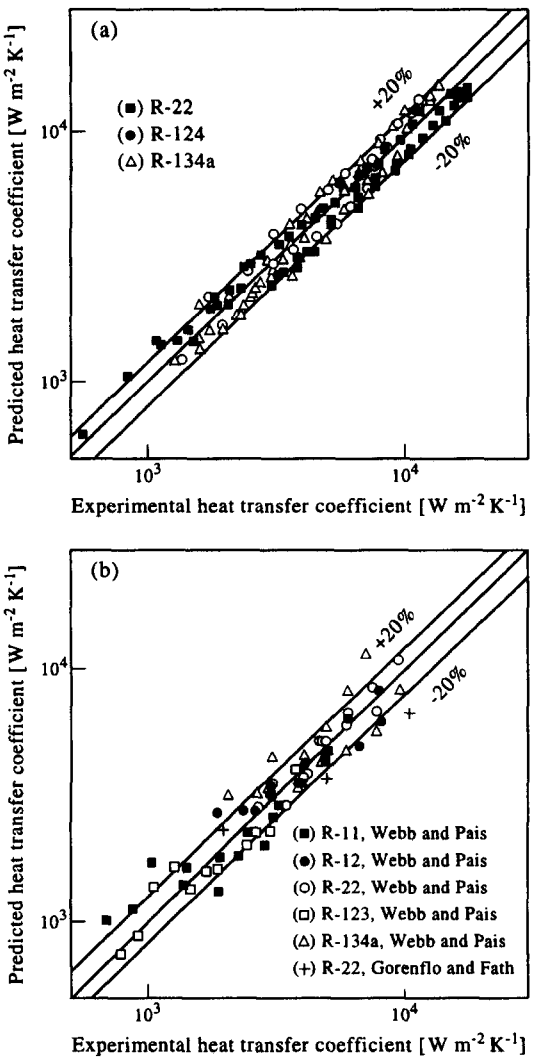

Fig. 8. Comparisons between the proposed prediction method and (a) the present experimental data; (b) the experimental data from refs. [7] and [22].

vection. The net result is a maximum phenomenon for the natural convection component. In the present investigation, the 'influence area' ratio is taken to be 4 as suggested by Hsu and Graham [21].

For a lower reduced pressure ($P_r = 0.01$), the distributions of the transient conduction, latent heat, and natural convection are quite different from those at higher reduced pressure. The effect of natural convection generally cannot be omitted, and both of the transient conduction and latent heat increases significantly with the wall superheat. However, the ratio, q_e''/q_t'', decreases with the wall superheat, and the latent heat contribution may be discarded for a heat flux over 10 000 W m^{-2}. Figure 7(b) shows the heat transfer rate for the individual contribution of transient conduction, latent heat transfer, and natural convection at a reduced pressure of 0.2 and of 0.004 for water. As seen, the distributions of these heat transfer components for water is analogous to those of R-123.

Figure 8(a) and (b) shows the predictions for the proposed method with the present experimental data, and the experimental data of R-11, R-12, R-22, R-123 and R-134a from Webb and Pais [7] and of R-22 from Gorenflo and Fath [22]. As shown in Fig. 8(a), the present method can predict 95% of the experimental data within 20%. In addition, based on the present experimental data bank, the proposed method can also predict the experimental data from Webb and Pais [7] and Gorenflo and Fath [22] with reasonably good accuracy as depicted in Fig. 8(b). Actually, 75% of the experimental data can be predicted within 20%.

CONCLUSIONS

(1) Pool boiling data for R-22, R-124 and R-134a on a plain tube are reported at saturation temperatures of 4.4°C and 26.7°C and at reduced pressures of 0.1 and 0.2. For a given saturation tempera-

ture, the heat transfer coefficient for R-124 is the smallest due to its low reduced pressure. Also, it is shown that the Cooper [8] correlation can predict the present pool boiling heat transfer quite satisfactorily.

(2) A modified Blöchl [5] method is proposed in this study; this semi-analytical model not only can predict the present data with success but also predict the experimental data from Webb and Pais [7] and of R-22 from Gorenflo and Fath [22] with reasonably good accuracies.

(3) The modified Blöchl [5] method suggests that the governing heat transfer mechanism depends on the reduced pressure and wall superheat. For a reduced pressure greater than 0.2, the natural convection is almost negligible, and the dominant heat transfer mechanism is latent heat transport instead of transient conduction. However, for a reduced pressure of 0.01, the contribution of natural convection generally cannot be omitted, and the contribution of transient conduction is higher than that of the latent heat. In addition, the transient conduction becomes the controlling heat transfer mechanism at higher wall superheat.

REFERENCES

1. Stephan, K. and Abdelsalam, M., Heat transfer correlations for natural convection boiling. *International Journal of Heat and Mass Transfer*, 1980, **23,** 73–87.
2. Cooper, M. G., Heat flow rates in saturated nucleate pool boiling—a wide-ranging examination using reduced properties. *Advances in Heat Transfer*, 1984, **16,** 157–239.
3. Kolev, N. I., How accurate can we predict nucleate boiling. *Experimental Thermal and Fluid Science*, 1995, **10,** 370–378.
4. Mikic, B. B. and Rohsenow, W. M., A new correlation of pool-boiling data including the effect of heating surface characteristics. *Journal of Heat Transfer*, 1969, **91,** 245–250.
5. Blöchl, R., Zum Einfluß der Oberflächenstruktur unterschiedlich bearbeiteter Heizflächen auf die Wärmeübertragung beim Blasensiden. Ph.D. dissertation, University of Karlsruhe, 1986.
6. Moffat, R. J., Describing the uncertainties in experimental results. *Experimental Thermal and Fluid Science*, 1988, **1,** 3–17.
7. Webb, R. L. and Pais, C., Nucleate pool boiling data for five refrigerants on plain, integral-fin and enhanced tube geonertries. *International Journal of Heat and Mass Transfer*, 1992, **35(8),** 1893–1904.
8. Cooper, M. G., Saturation nucleate pool boiling—a simple correlation. *International Chemical Engineering Symposium Series*, 1984, **86,** 785–792.
9. Mostinski, I. L., Calculation of heat transfer and critical heat flux in boiling liquids based on the law of corresponding states. *Teploenergetika*, 1963, **10,** 66–71.
10. Tong, W., Bar-Cohen, A. and Simon, T. W., Thermal transport mechanisms in nucleate pool boiling of highly-wetting liquids. In *Ninth International Heat Transfer Conference*, Vol. 2, 1990, pp. 27–32.
11. Bayley, F. J., An analysis of turbulent free convection heat transfer. *Proceedings of the Institute of Mechanical Engineering*, 1955, **169,** 361.
12. Cole, R. and Rohsenow, W. M., Correlation of bubble departure diameters for boiling of saturated liquids. *Chemical Engineering Progress Symposium Series*, 1966, **65,** 6–16.
13. Zuber, N., Hydrodynamic aspects of boiling heat transfer. U.S. AEC Report, AECU 4439, 1959.
14. Griffith, P. and Walis, G. D., The role of surface conditions in nucleate boiling. *Chemical Engineering Progress Symposium Series*, 1960, **56,** 49–63.
15. Judd, R. L. and Shouki, M., Nucleate boiling on an oxide coated glass surfaces. *ASME Journal of Heat Transfer*, 1975, **97,** 494–495.
16. Fujita, Y., Ohta, H., Hidaka, S. and Nishikawa, K., Nucleate boiling heat transfer on horizontal tubes in bundles. In *Eighth International Heat Transfer Conference*, 1986, Vol. 5, pp. 2131–2136.
17. Bier, K., Gorenflo, M. and Salem, M., Size distribution of surface cavities and of stable nuclei for pool boiling heat transfer to refrigerants. In *Fifteenth International Congress of Refrigeration*, Venice, Italy, 1979, paper B1–91.
18. Jamialahmadi, M., Blöchl, R. and Müller-steinhagen, H., Pool boiling heat transfer to saturated water and refrigerant 113. *The Canadian Journal of Chemical Engineering*, 1991, **69,** 746–754.
19. Yang, S. R. and Kim, R. H., A mathematical model of the pool boiling nucleation site density in terms of the surface characteristics. *International Journal of Heat and Mass Transfer*, 1988, **31,** 1127–1135.
20. Kocamustafagullari, G. and Ishii, M., Interfacial area and nucleation site density in boiling system. *International Journal of Heat and Mass Transfer*, 1983, **26,** 1377–1387.
21. Hsu, Y. Y. and Graham, R. W., NASA TN D-594, 1961.
22. Gorenflo, D. and Fath, W., Heat transfer at pool boiling outside of finned tubes at high saturation pressures. In *Proceedings of the Seventeenth International Congress of Refrigeration*, Wien, Vol. B, 1987, pp. 955–968.